

## **[Re<sub>2</sub>(μ-1,2,4-triazolate)<sub>2</sub>(μ-OH)(CO)<sub>6</sub>]<sup>-</sup>: a novel metalloligand for the construction of flexible porous coordination networks**

Elisa Barea,<sup>a</sup> Antonio Rodríguez-Diéguez,<sup>b</sup> Jorge A. R. Navarro,<sup>c</sup> Giuseppe D'Alfonso<sup>a</sup> and Angelo Sironi<sup>b</sup>

<sup>a</sup> *Dipartimento di Chimica Inorganica, Metallorganica e Analitica, Università degli Studi di Milano, Via Venezian 21, 20133 Milano.*

<sup>b</sup> *Dipartimento di Chimica Strutturale e Stereochimica Inorganica, Università degli Studi di Milano, Via Venezian 21, 20133 Milano.*

<sup>c</sup> *Departamento de Química Inorgánica, Universidad de Granada, Av. Fuentenueva S/N, 18071 Granada, Spain.*

### **Characterization and Physical Measurements.**

Elemental (C,H,N) analyses were obtained at a CHNS/O Perkin Elmer 2400 analyzer and <sup>1</sup>H NMR spectra were recorded on a Bruker DRX400 spectrometer (University of Milan); thermogravimetric analyses were registered on a NETZSCH STA 409 PC/PG equipment, at heating rate of 20 °C min<sup>-1</sup>, respectively (University of Insubria) in the presence of a dinitrogen atmosphere. Sorption isotherms were measured on a Micromeritics Tristar 3000 (University of Granada) volumetric instruments under continuous adsorption conditions. Prior to measurement, powder samples were heated at 60 °C for 2 h and outgassed to 10<sup>-3</sup> Torr using a Micromeritics Flowprep. X-ray powder diffractometric experiments were performed on a Bruker AXS Advance D8 diffractometer (University of Milan), by employing a background free sample holder. Typically, a sequence of scans in the 5-40° 2θ range was performed.

General characterization:

[Et<sub>4</sub>N]**2**. Anal. Calcd for Re<sub>2</sub>C<sub>18</sub>H<sub>25</sub>N<sub>7</sub>O<sub>7</sub>: C, 26.24; H, 3.06; N, 11.90. Found: C, 26.18; H, 3.05; N, 12.25. <sup>1</sup>H NMR (CD<sub>3</sub>CN, 298 K). δ (ppm) = 8.12 (s, 4 H); 3.18 (q, 8 H, J<sub>HH</sub> = 7.3 Hz, CH<sub>2</sub>CH<sub>3</sub>); 1.23 (tt, 12 H, J<sub>HH</sub> = 7.3 Hz, J<sub>HN</sub> = 1.8 Hz, CH<sub>2</sub>CH<sub>3</sub>). IR (CH<sub>3</sub>CN). ν (C=O, cm<sup>-1</sup>) = 2019 (vw), 2007 (vs), 1900 (vs), 1886 (s).

**Ag@2.** Anal. Calcd for  $\text{AgRe}_2\text{C}_{10}\text{H}_5\text{N}_6\text{O}_6 \cdot (\text{CH}_3\text{OH})_{0.33}$ : C, 15.59; H, 0.80; N, 10.56. Found: C, 15.42; H, 0.80; N, 10.54.

**Ag@2D.** Anal. Calcd for  $\text{AgRe}_2\text{C}_{10}\text{H}_5\text{N}_6\text{O}_6 \cdot ((\text{CH}_2\text{CH}_2\text{OH})_2\text{O})_{1.5}$ : C, 20.00; H, 2.10; N, 8.75. Found: C, 19.89; H, 2.17; N, 9.08.

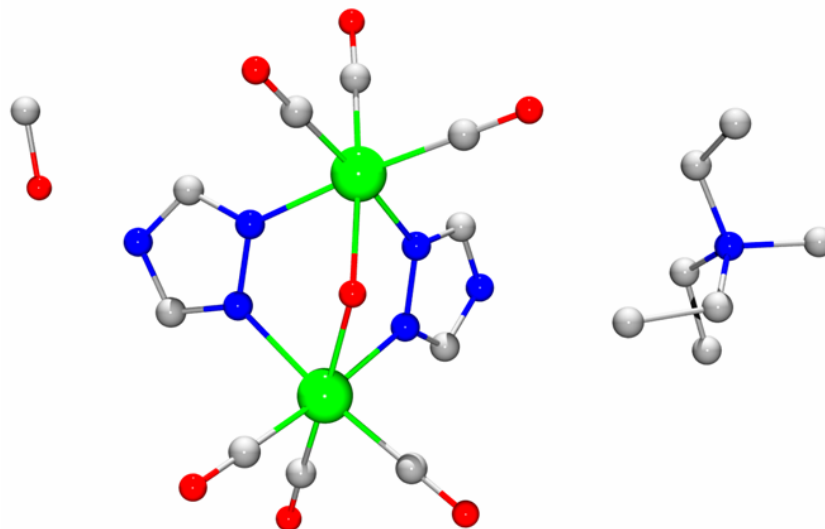


**Fig. S1** Asymmetric unit in  $\{[\text{Et}_4\text{N}][\text{Re}_2(\mu\text{-trz-}\kappa\text{N}^1:\kappa\text{N}^2)_2(\mu\text{-OH})(\text{CO})_6]\}_n \cdot n\text{CH}_3\text{OH}$ . Re (green), C (grey), N (blue), O (red).

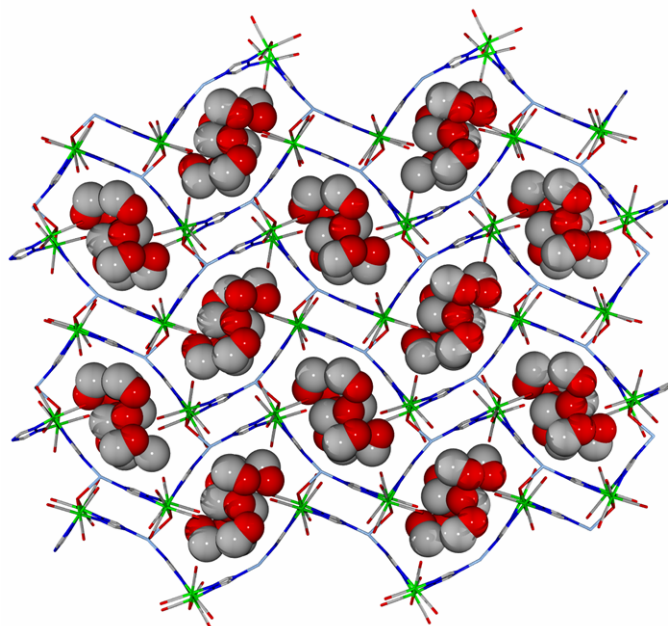


**Fig. S2** Perspective view of one of the layers containing solvation MeOH molecules in the  $\text{Ag}_4(\text{Re}_2)_4$  voids. Re (green), Ag (light blue), C (grey), N (blue), O (red).

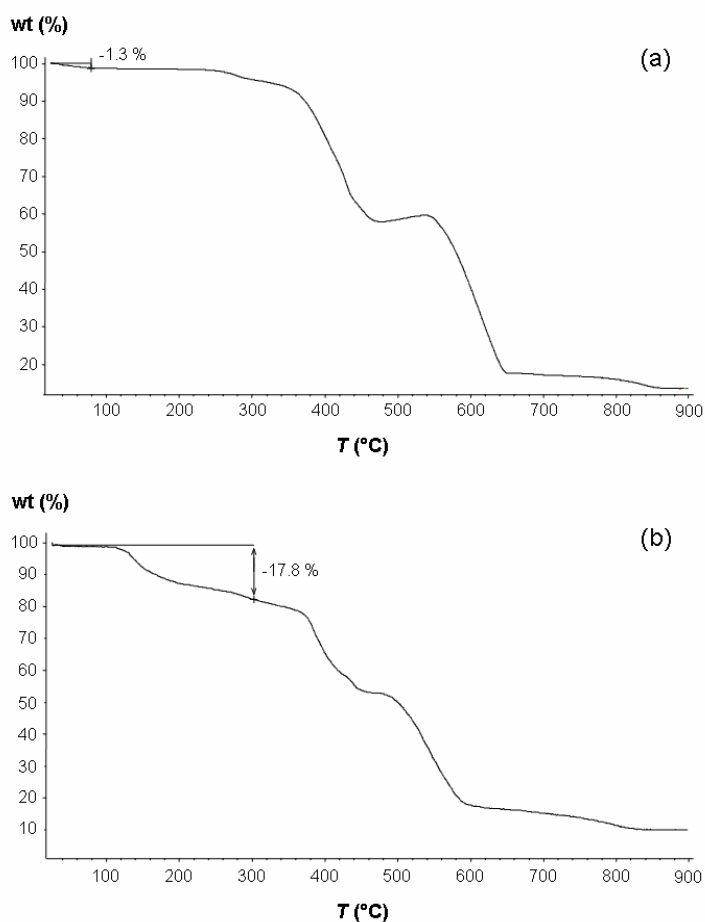


**Fig. S3** TGA curves of (a)  $\text{Ag@2}$  (calc. per 0.33 MeOH molecules, -1.3 %; found, -1.3 %) and (b)  $\text{Ag@2D}$  (calc. per 1.5  $(\text{CH}_2\text{CH}_2\text{OH})_2\text{O}$ ) molecules, -16.6 %; found, -17.8 %).

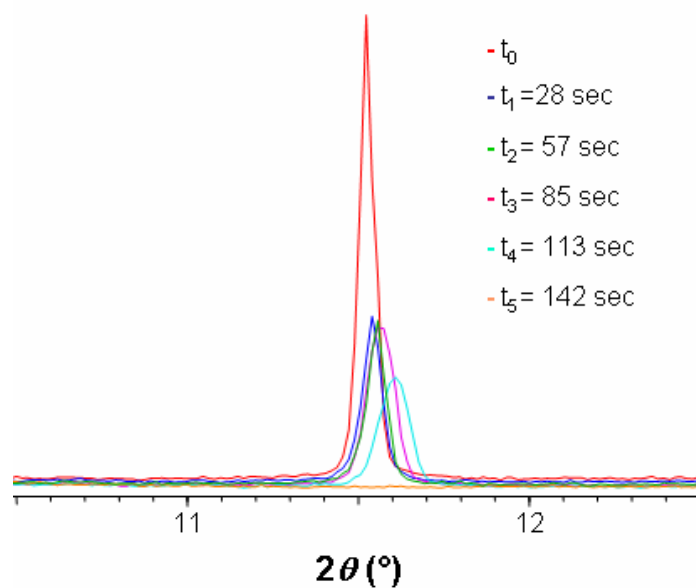


**Fig. S4** Evolution of the XRPD traces of  $\text{Ag@2}_M$  during desolvation in the  $10.5\text{-}12.5^\circ$  range, collected using a Position Sensitive Detector with a window of  $2^\circ$  on a drop of  $\text{Ag@2}_M$  slurry deposited on a free background sample holder. It can be observed that the 020 reflection of the solvated phase disappears in only 2.5 minutes.

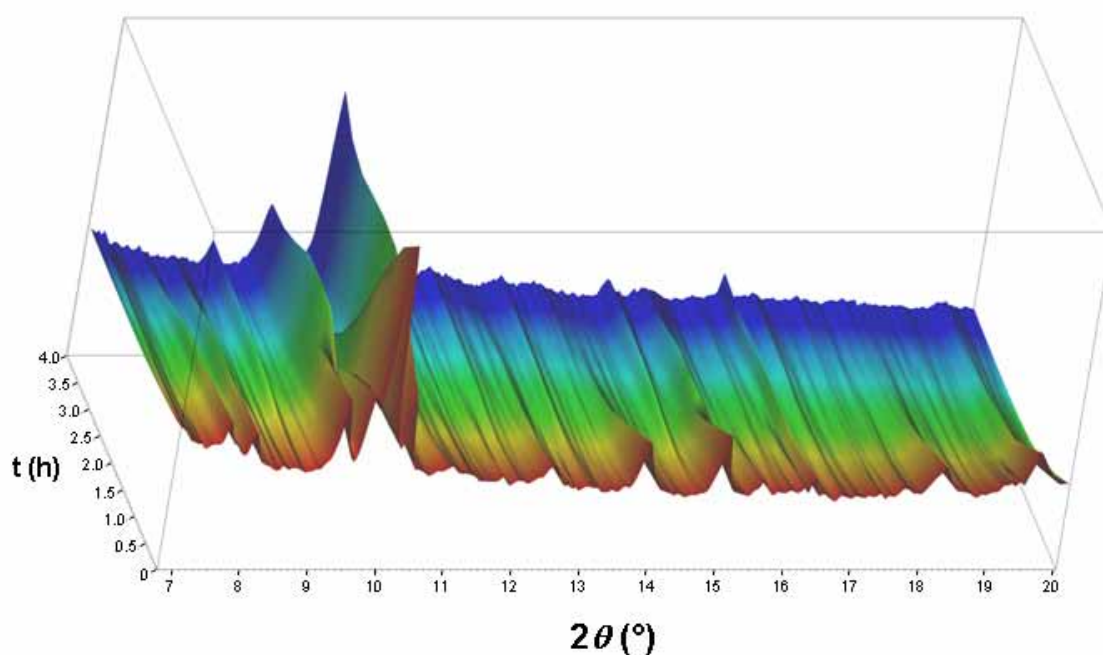


**Fig. S5** Evolution of the XRPD diffractograms during the  $\text{Ag@2}_E \leftrightarrow \text{Ag@2}'$  transformation. In this case, it should be noted that the desolvation process occurs in a few hours and not in a few seconds as in  $\text{Ag@2}_M$ . A drop of  $\text{Ag@2}_E$  slurry was deposited on a free background sample holder and, then, we started to record a set of XRPD patterns ( $5\text{-}40^\circ$   $2\theta$ , step  $0.02^\circ$ , 1s per step). The  $t_0$  diffractogram corresponds to the first trace lacking of the solvent bump.

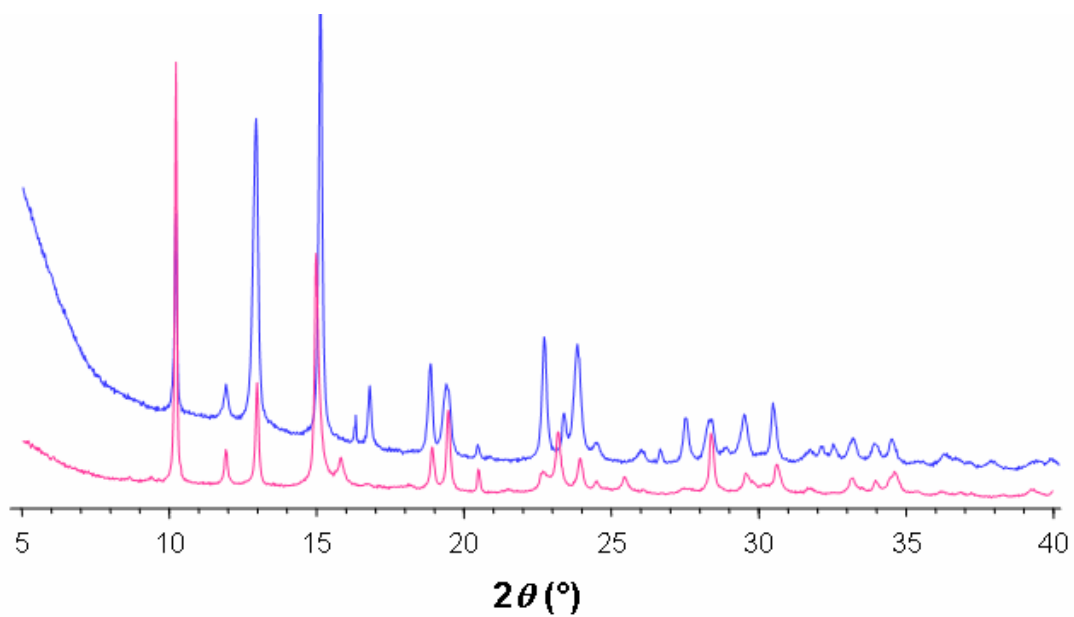


**Fig. S6** XRPD traces of the desolvated  $\text{Ag@2}$  (blue) and  $\text{Ag@2'}$  (pink) phases.

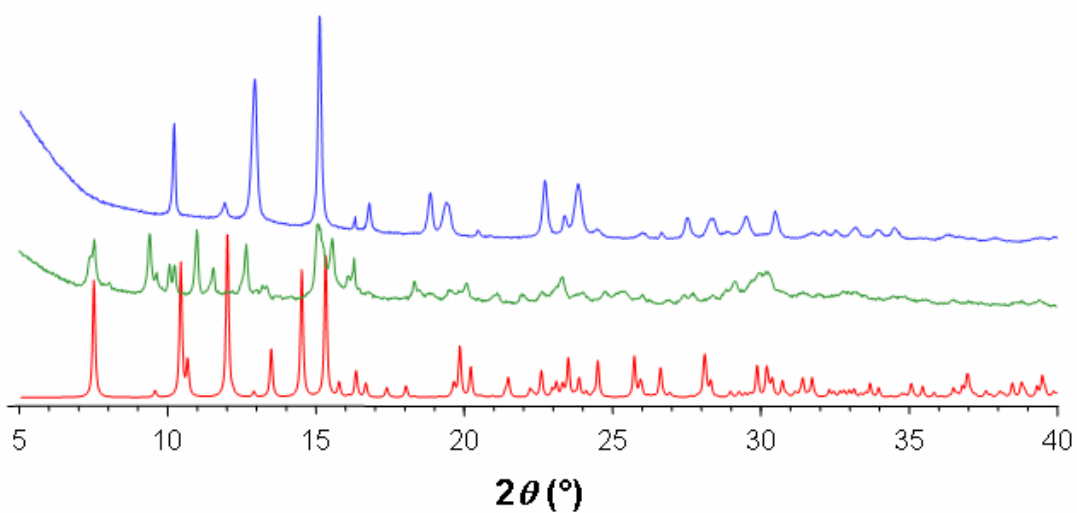


**Fig. S7** XRP diffractogram of  $\text{Ag@2D}$  (green) in comparison with the XRPD traces of the  $\text{Ag@2}$  phase (blue) and the simulated spectrum of  $\text{Ag@2M}$  (red).

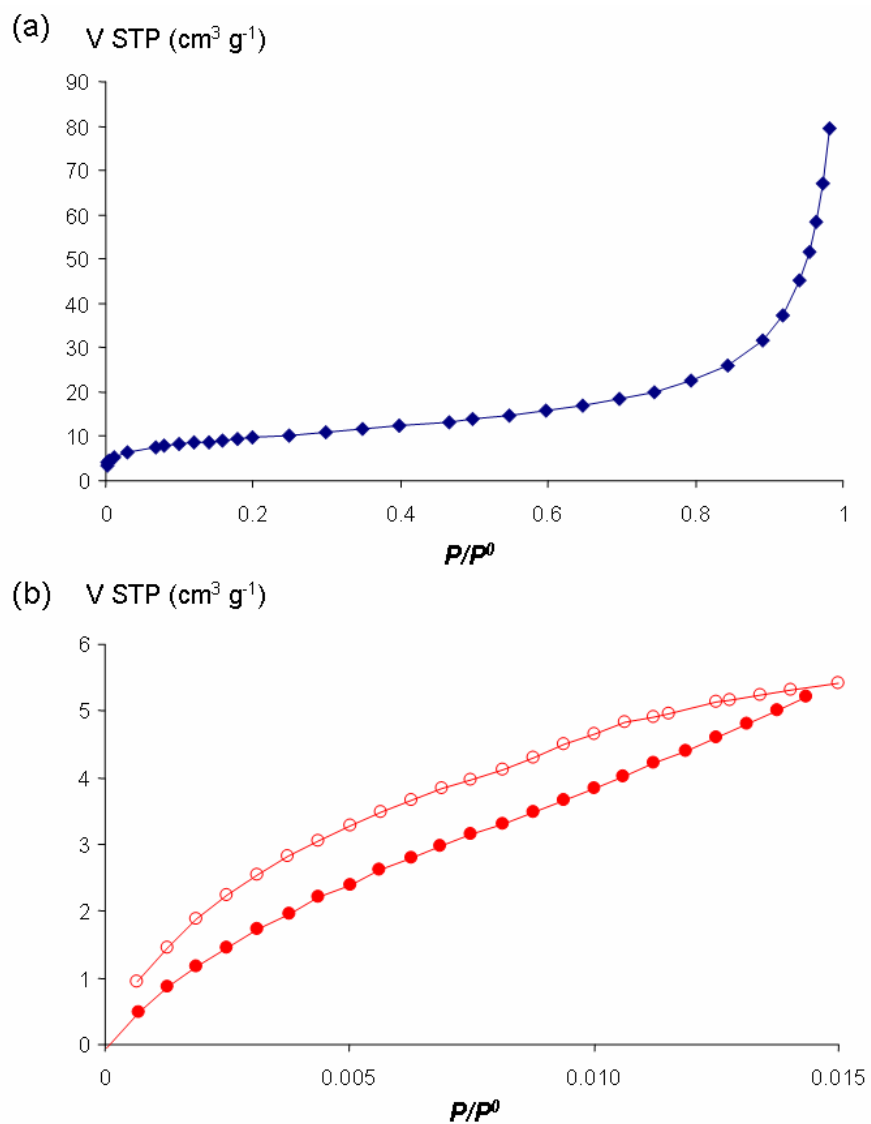


**Fig. S8**  $\text{N}_2$  (a) and  $\text{CO}_2$  (b) sorption isotherms of  $\text{Ag}@2$  measured at 77 and 293 K, respectively. The open symbols denote desorption.